Suppression of Wave-Breaking in Nonlinear Water Wave Computations

Anil K. Subramani, Robert F. Beck, and William W. Schultz
The University of Michigan, Ann Arbor, Michigan 48109, U.S.A.

INTRODUCTION

Over the past several years, a multipole-accelerated, desingularized boundary integral method has been developed to compute fully nonlinear water waves in the time domain (Scorpio and Beck, 1996). The method---denominated UM-DELTA, for University of Michigan Desingularized Euler-Lagrange Time-Domain Approach---has been successfully applied to a wide variety of problems, with marked improvements over results obtained using linearized methods. A major difficulty is encountered, though, by this and similar methods for computing nonlinear water waves and wave loads: the characteristic occurrence of spray and wave-breaking in free-surface flows causes the computations to stop, as figure 1 demonstrates. Therefore, for the present method to realize its full capability, it is important to prevent the generation of spray and breaking waves from terminating the simulations of highly nonlinear flows. However, with the goal being for the method to remain efficient and useful in the marine design process, a detailed and expensive simulation of the wave-breaking event itself is less desirable an approach than one that models the event adequately enough for the calculations to proceed.

To this end, recognizing that wave-breaking is essentially a process with which is associated a local dissipation of energy, a technique is herein proposed to absorb energy locally from waves that are about to break, thereby suppressing wave-breaking. The features of this "local absorbing patch" model are: (i) detecting the likely occurrence of wave-breaking, and (ii) determining the appropriate amount of local damping so as to render reasonably realistic waves in the post-breaking regime; these are discussed below.

CRITERION FOR BREAKING

Important as the problem is, wave-breaking has received considerable attention, but it is not yet completely understood. A survey of the literature reveals that a number of studies have been conducted to understand why waves break and to determine a reliable criterion for the inception of breaking. For brevity, we cite only Griffin et al. (1994) for they point to the pertinent references in their review of the existing criteria.

Following Stokes' theorizing of a limiting height (H) to a wave in terms of the wavelength (λ), the wave steepness (often measured by ak, where a is the wave amplitude and $k=2\pi/\lambda$ is the wave number) has been the most commonly examined index for wave-breaking. Empirical data, however, show the steepness to be an imprecise criterion---see figure 1 and table 1 of Griffin et al., 1994, which indicate that waves break at lower steepnesses than that suggested by Stokes' criterion and also show the scatter in the data. Another widely pursued idea has been the prescribing of a limiting value to the fluid velocity at a crest. For example, recently, Wang et al. (1994) provided data obtained from a two-dimensional numerical wave tank in support of the criterion that a wave breaks when the horizontal particle velocity reaches the local group velocity. The possibility of breaking has also been related to the energy content in the waves, by others, but these last two criteria are difficult to extend to three-dimensional flows. Criteria based on the wave slope and accelerations of the free-surface have also been suggested, but the consensus is that none of the above constitutes a simple, precise, and universally valid criterion.

In this light, we pursue a criterion based on the wave steepness because of its simplicity and its applicability in three-dimension. A steepness criterion that requires an estimate of the local wavelength, however, is not easy to implement, especially when waves of different frequencies are present and interact. We exploit instead that when waves break---or are about to---they attain a profile with a sharp crest of infinite curvature (κ). Furthermore, empirical studies of steep but non-breaking regular waves indicate that waves that do not possess a sharp crest obey the approximate non-dimensional bound, $|\kappa\lambda| \leq 6$. Figure 2 depicts how this applies to waves of steepness, $H/\lambda \approx 1/12$, whose leading front went on to break. We therefore seek to use the exceeding of this bound---as when any wave steepens to a sharp crest---as a "trigger" for the activation of a localized wave damper in the fully nonlinear computations.

To implement the idea, we then proceed to reformulate the steepness criterion in terms of a limiting value of κa: Adopting the approximate criterion that a wave breaks when its steepness, H/λ exceeds 1/12 and using the above bound on $|\kappa\lambda|$, we obtain the condition, $|\kappa H| \leq 0.5$ for a wave not to break. We convert this into one based on κa since the crest-to-trough wave-height is not as easily available; we do so on the basis of the observable geometric property of incipient breaking waves that $a \approx 0.7$ H on

an average (e.g., Bonmarin, 1989), obtaining, finally, $|\kappa a| \leq 0.35$.

In order to examine the reliability of this curvature-based criterion, regular, deep-water gravity waves of varying steepnesses (as generated in a two-dimensional wave tank by a wedge wave-maker) were simulated, and the variation of $|\kappa a|$ with the steepness, ak was noted. (Note that, in the evaluation of the abscissas, the nominal wavelength given by $k = \omega^2/g$ was used.) This variation is depicted in figure 3; for comparison, that for a second-order Stokes wave is also presented. For all waves of steepness, ak less than about 0.25, the prescribed threshold value of $|\kappa a| = 0.35$ is never exceeded. For higher ak, this limit is exceeded at times by waves that attain a sharp crest, especially at the leading wave front. Not all waves that do so go on to break; therefore, the present threshold poses a conservative, if imprecise limit. However, a conservative criterion is necessary to ensure that all likely instances of breaking are detected so that they may be suppressed.

Although some of the scatter in the data in figure 3 is due to the non-uniformities in fully nonlinear waveforms, it is largely due to the inevitable noise in the numerical evaluation of the curvature. We compute the curvature using a local three-point formula arising from the fitting of a circle through three consecutive free-surface nodes---a formula that does give agreeable results with the analytically obtained curvatures for smoother profiles. Nonetheless, this scatter does not appear to affect the nature of the $|\kappa a| - ak$ curve or the limiting $|\kappa a|$ value considerably.

Finally, the sensitivity of the curvature computations to the fineness of the node distribution was studied through a convergence study: The curvature of the free-surface was computed for one particular case of wave-maker motion amplitude and frequency (the resulting waves had a steepness of about ak=0.21) using three different node distributions---25, 50, and 100 nodes per wavelength (the usual distribution adopted---the minimum recommended---is 30 nodes per wavelength; the results presented in figures 2 and 3 were obtained using 40 nodes per wavelength). A sample comparison of the results is presented in figure 4. Notice that although there is a lot more noise in the calculations as the node density increases, the important maximum values of the curvature do not change much between the three cases.

Thus, we have arrived at a curvature-based criterion for breaking that is simple and easy to implement, even when waves of different frequencies are present. The mechanism by which energy is absorbed locally from the waves when this criterion is met is discussed in the next section.

SUPPRESSION OF A BREAKING WAVE

We employ a variation of the numerical absorbing beach used by Cao et al. (1993), in order to suppress wave-breaking locally; the basic idea, though, is the same---it consists of exerting an additional, external pressure on the wave in the vicinity of the location where the likelihood of wave-breaking has been detected. By causing the wave to work against this external pressure, the energy necessary to prevent the wave from breaking is extracted locally from the fluid (hence, "local absorbing patch"). Mathematically, this consists of the inclusion of an additional term, P_{damp}, in the dynamic free-surface boundary condition:

$$\frac{\partial \phi}{\partial t} + \frac{1}{2}\nabla\phi.\nabla\phi + \frac{p}{\rho} + gz + \frac{P_{damp}}{\rho} = 0.$$

Note that P_{damp} is non-existent outside the absorbing patch; within the patch, we prescribe the following form to the damping term:

$$P_{damp} = \sigma\, \nu(x)\, |\nabla\phi|^2\, \mathrm{sgn}\left(\frac{\partial \phi}{\partial n}\right)$$

The $|\nabla\phi|^2$ term determines the magnitude of the damping; σ is a coefficient that may be varied to increase or decrease the amount of damping; the signum function ensures that the pressure is acting against the wave; and $\nu(x)$ is a shape function chosen to ensure that the damper takes the form of a smoothly varying patch:

$$\nu(x) = 0.5\left(1 + \cos\left(\frac{\pi(x - x_o)}{L_o}\right)\right)$$

Here, x_o is the location where $|\kappa a| = 0.35$ is exceeded, and L_o is half the length, centered about x_o, over which the damper acts. We prescribe L_o to be $a_o/0.35$ (a_o is the wave amplitude at x_o)---again, from considerations of the geometry of breaking waves, so that the energy is extracted from approximately the portion of the wave between zero-crossings.

RESULTS

The effectiveness of the present "local absorbing patch" model is demonstrated by application to the breaking wave encountered in figure 1. As shown in figure 5, the wave-breaking is successfully detected and suppressed sufficiently for the calculations to proceed. The strength of the damping constant used was σ=12.5. An uncertainty with the present model, however, is that the amount of damping required to suppress

wave-breaking is not easily determined---some other calculations have required larger values of σ (of about 25) to suppress the wave-breaking. Moreover, it may well be that for extreme cases suppressing the tendency of waves to break while obtaining reasonable results in the post-breaking regime is an impossible task. These call for additional investigations.

The effects of prescribing a σ greater than that which is necessary to suppress the breaking may be small, as the results plotted in figure 6 suggest. Therein, a comparison is made of the calculations presented in figures 1 and 5 and an additional calculation obtained using damping equivalent to σ=25. Not only does the plot clearly show the difference in the wave profile due to the extraction of the energy associated with the breaking, but also, the difference in the calculations obtained with the two different damping strengths is imperceptible. This is due to the feature of the model that damping is present only when triggered by high values of $|\kappa a|$ ($|\kappa a|$ greater than 0.35) and only as long as $|\kappa a|$ is above the threshold value.

The present model therefore holds much promise for extending fully nonlinear water wave computations into the important highly nonlinear regime. An important step involves the validation of the post-breaking calculations against experimental data, which we are currently seeking. Efforts are also underway to develop a strategy for extending the model to three-dimensional flow computations. A proposed approach, especially for ship-flow calculations, is to detect the occurrence of and suppress wave-breaking along prescribed free-surface paths (these are the paths on which the Lagrangian nodes are convected in the UM-DELTA method; they generally take the appearance of free-surface streamlines).

Future work will involve the extensive testing of the model over a wide variety of breaking wave conditions. We also plan to compute the total energy in the fluid domain and the fraction of the total energy that is absorbed by the wave damper. We hope to relate the computed energy losses to the numerous experimental studies of wave-breaking.

ACKNOWLEDGEMENTS

This research was funded by the Office of Naval Research and the University of Michigan--Sea Grant--Industry Consortium on Offshore Engineering. The computations were supported by allocations of high performance computing resources through the U.S. Department of Defense High Performance Computing Modernization Program and the National Partnership for Advanced Computational Infrastructure. We thank Mr. Eirik Malthe-Sorenssen for his assistance with some of the calculations.

REFERENCES

Bonmarin, P., "*Geometric Properties of Deep-Water Breaking Waves," Journal of Fluid Mechanics*, Vol. 209, 1989, pp. 405-433.

Cao, Y., Beck, R.F., and Schultz, W.W., "*An Absorbing Beach for Numerical Simulations of Nonlinear Waves in a Wave Tank*," Proceedings, Eighth International Workshop on Water Waves and Floating Bodies, Newfoundland, Canada, 1993.

Griffin, O., Peltzer, R., Wang, H., and Schultz, W., "*Kinematic and Dynamic Evolution of Deep Water Breaking Waves*," Proceedings, Twentieth Symposium on Naval Hydrodynamics, Santa Barbara, U.S.A., 1994.

Scorpio, S.M. and Beck, R.F., "*A Multipole Accelerated Desingularized Method for Computing Nonlinear Wave Forces on Bodies*," Proceedings, Fifteenth Offshore Mechanics and Arctic Engineering Conference, Florence, Italy, 1996; also, to appear in the Journal of Offshore Mechanics and Arctic Engineering.

Wang, P., Yao, Y., and Tulin, M.P., "*Wave Group Evolution, Wave Deformation, and Breaking: Simulation Using LONGTANK*, a Numerical Wave Tank," International Journal of Offshore and Polar Engineering, Vol. 4, No. 2, 1994.

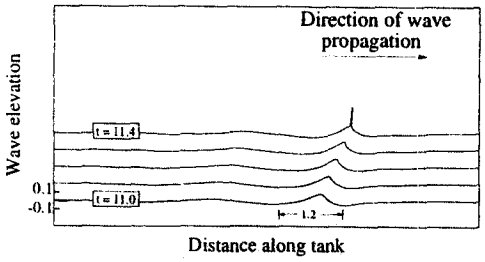

Figure 1. Time-history of the surface displacement in a numerical simulation, using UM-DELTA, of shallow-water waves generated by a piston wave-maker in a two-dimensional wave-tank. The calculations cease at about t=11.4 due to the occurrence of a breaking wave caused by the coalescing of waves of different frequencies.

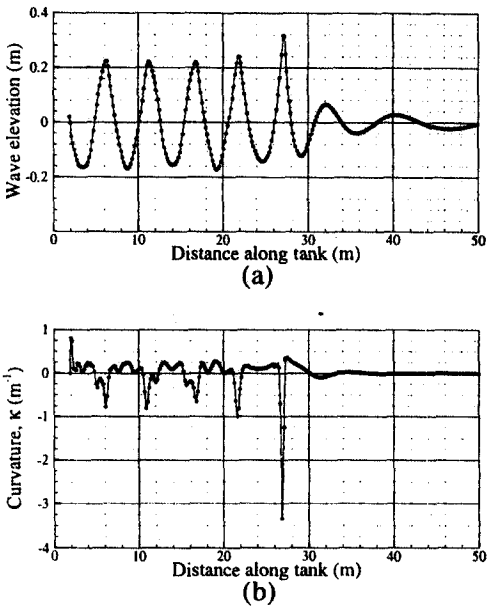

Figure 2. A representative snapshot at t=18.8 of: (a) the surface displacement, and (b) the curvature of the surface, for waves as generated by a wedge wave-maker of motion amplitude 0.12m and frequency 0.559Hz (nomimal λ=5m). The leading wave front broke at about t=23.3 in this simulation. Note that for the other wave crests, $|\kappa\lambda| \leq 6$, approximately.

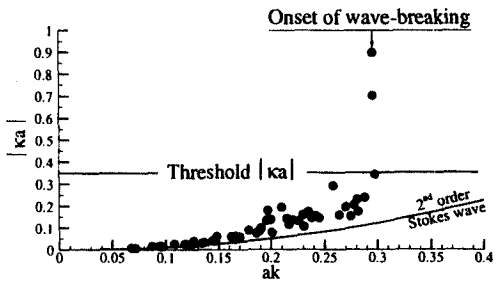

Figure 3. Observed variation with wave steepness, ak, of the proposed wave-breaking index, $|\kappa a|$, for regular, deep-water gravity waves. The variation for a 2nd order Stokes wave is presented for comparison.

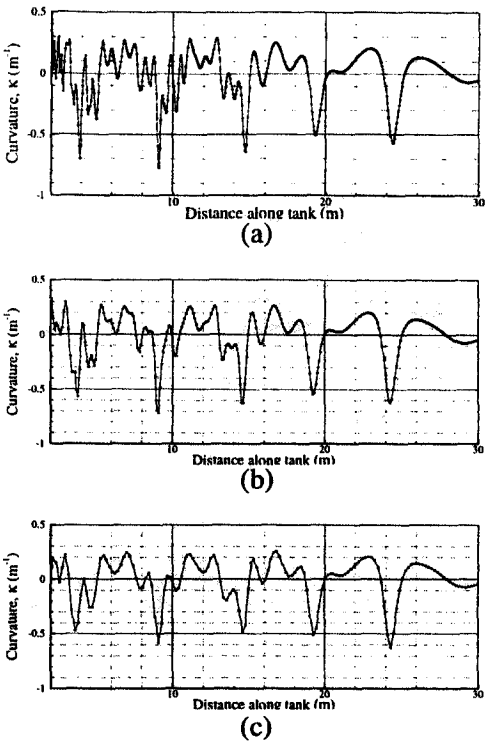

Figure 4. A representative snapshot of the computed curvature of the surface (for waves generated by a wedge wave-maker of motion amplitude 0.08m and frequency 0.559Hz), using: (a) 100 nodes per wavelength, (b) 50 nodes per wavelength, and (c) 25 nodes per wavelength.

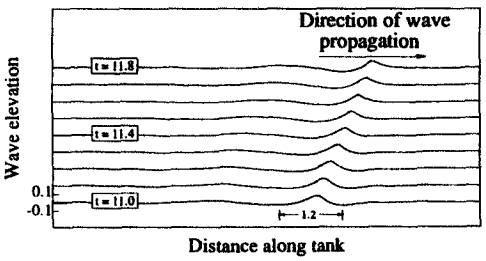

Figure 5. Time-history of the surface displacement in a repeat of the numerical simulation shown in figure 1, but differing (only) in that a "local absorbing patch" model has been implemented. The model detects the likely occurrence of and suppresses the wave-breaking.

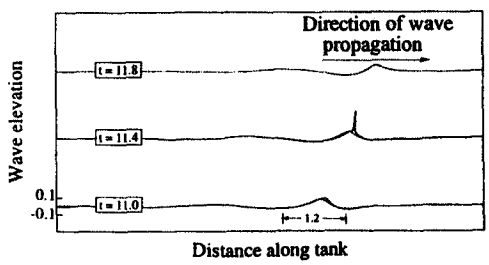

Figure 6. Time-history of the surface displacement in simulations involving: no damping (solid line); damping with σ=12.5 (dashed line); and damping with σ=25 (dotted line).